

Classification of phase transitions in small systems

Peter Borrmann and Oliver Mülken

Department of Physics, Carl von Ossietzky University Oldenburg, D-26111 Oldenburg, Germany
(February 20, 2019)

We present a classification scheme for phase transitions in finite systems like clusters or nuclear matter based on the Lee-Yang zeros in the complex temperature plane. In the limit of infinite particle numbers the scheme reduces to the Ehrenfest definition of phase transitions and gives the right critical indices. We apply this classification scheme to small noble gas clusters and Bose-Einstein condensates in a harmonic trap as examples of analogues of first and second order phase transitions in finite systems.

PACS numbers: 05.70.Fh, 64.60.Cn, 64.70.-p

Small systems do not exhibit phase transitions. Following Ehrenfest's definition this statement is true for almost all small systems. Instead of exhibiting a sharp peak or a discontinuity in the specific heat at some well defined critical temperature the specific heat shows a hump extending over some finite temperature range. For example for melting of atomic clusters this is commonly interpreted as a temperature region where solid and liquid clusters coexist [1,2] and as a finite-system analogue of a first order phase transition. Proykova and Berry [3] interpret a structural transition in TeF_6 clusters as a second order phase transition. A common way to investigate if a transition in a finite system is a precursor of a phase transition in the corresponding infinite system is to study the particle number dependence of the appropriate thermodynamic potential [4]. However, this approach will fail for all system types where the nature of the phase transition changes with increasing particle number which seems to be the case e.g. for sodium clusters [5] or ferrofluid clusters [6]. For this reason a definition of phase transitions for systems with a fixed and finite particle number seems to be desirable. The only recommended feature is that this definition should reduce to the Ehrenfest definition when applied to infinite systems.

Our ansatz presented in this Letter is based on earlier works of Lee and Yang [7,8] and Grossmann *et al.* [9–11] who gave a description of phase transitions by analysing the distributions of zeros (DOZ) of the grandcanonical $\Xi(\beta)$ and the canonical partition function $Z(\beta)$ in the complex temperature plane. In the following we denote complex temperatures by $\mathcal{B} = \beta + i\tau/\hbar$ where β is as usual $1/k_B T$ and τ has the dimension of time. For macroscopic systems this analysis merely contributes a sophisticated view of the thermodynamic behavior of the investigated system. Grossmann *et al.* conclude, that for cases, where the distribution of zeros is given by simple lines in the complex plane, the order of the phase transition and the

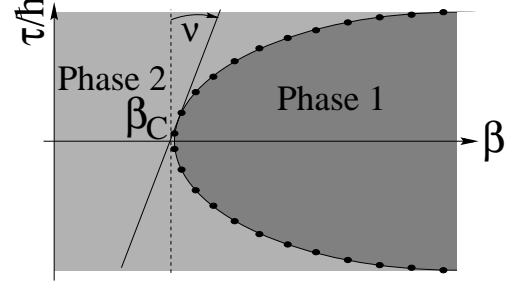


FIG. 1. Density of zeros in the complex temperature plane.

critical exponents can be extracted from the behaviour of these lines close to the critical temperature β_c , specifically from the density of zeros $\Phi(\tau, \gamma)$ on these lines and the crossing angle $\nu = \arctan(\gamma)$ of these lines with the real temperature axis (see Fig. 1). Assuming that for small τ the density of zeros $\Phi(\tau, \gamma)$ can be approximated by a simple power law $\Phi \approx \tau^\alpha$ the parameter set (α, γ) is sufficient to describe the phase transition. In the case $(\alpha \leq 1, |\gamma| \leq 1)$ a first order phase transition occurs, while in the case $(\alpha > 1, \gamma \text{ arbitrary})$ the phase transition is of higher order.

The free energy $F = -\frac{1}{\beta} \ln(Z(\mathcal{B}))$ is holomorphic everywhere in the complex temperature plane except at the zeros of Z . If the lines of zeros are dense in the complex plane, different phases are represented by the different regions of holomorphy of F and separated by the lines of zeros in the complex temperature plane. Ehrenfest phase transitions only occur where lines of zeros cross the real axis.

We will show that for small systems the distributions of zeros are able to reveal the secrets of small systems in a distinct manner. In the following we restrict our discussion to the canonical ensemble [12]. In the case of finite systems one must not deal with special considerations regarding the thermodynamic limit and the theorem of Mittag-Leffler [13] can directly be used to write down the canonical partition function as a function of the zeros in the complex plane

$$Z(\mathcal{B}) = Z(0) \exp \left(\mathcal{B} \frac{\partial_{\mathcal{B}} Z(0)}{Z(0)} \right) \times \prod_{k \in \mathbb{N}} \left(1 - \frac{\mathcal{B}}{\mathcal{B}_k} \right) \left(1 - \frac{\mathcal{B}}{\mathcal{B}_k^*} \right) \exp \left(\frac{\mathcal{B}}{\mathcal{B}_k} + \frac{\mathcal{B}}{\mathcal{B}_k^*} \right). \quad (1)$$

Because $Z(\mathcal{B})$ is an integral function the zeros $\mathcal{B}_k = \mathcal{B}_{-k}^* = \beta_k + i\tau_k/\hbar$ ($k \in \mathbb{N}$) of Z are complex conjugated, which is reflected in eq.(1). The DOZ contains the complete thermodynamic information about the system and

all desired thermodynamic functions are derivable from it. The internal energy U and the specific heat C_V are calculated by standard differentiation and yield

$$U = U^{\text{lim}} + 2 \sum_{k \in \mathbb{N}} \frac{\beta_k - \beta}{(\beta_k - \beta)^2 + \tau_k^2 / \hbar^2} - \frac{\beta_k}{\beta_k^2 + \tau_k^2 / \hbar^2} \quad (2)$$

and

$$C_V = C_V^{\text{lim}} - 2\beta^2 \sum_{k \in \mathbb{N}} \frac{(\beta_k - \beta)^2 - \tau_k^2 / \hbar^2}{((\beta_k - \beta)^2 + \tau_k^2 / \hbar^2)^2}, \quad (3)$$

where U^{lim} and C_V^{lim} are the appropriate infinite temperature limits ($\beta = 0$). As can be seen from equation (3) a zero approaching the real temperature axis infinitely close causes a divergence in the specific heat.

We now restrict our discussion to classical systems but all arguments given below apply equally well to quantum systems. The classical partition function in the complex temperature plane is given by

$$Z_N(\mathcal{B}) = \int \frac{d^{3N}p d^{3N}x}{N! \hbar^{3N}} \exp(-\mathcal{B}\mathcal{H}(p, x)) \quad (4)$$

Integrating out the momentum part yields

$$\begin{aligned} Z_N(\mathcal{B}) &= \left(\frac{1}{\mathcal{B}}\right)^{3N/2} \int d^{3N}\mathbf{x} \exp(-\mathcal{B}V(\mathbf{x})) \\ &= \left(\frac{1}{\mathcal{B}}\right)^{3N/2} \int dE \rho(E) \exp(-\mathcal{B}E), \end{aligned} \quad (5)$$

where $V(\mathbf{x})$ is the classical N -particle potential and $\rho(E)$ is the density of states with potential energy E . Having the density of states at hand the zeros of Z can be found by standard numerical methods.

Before stating our proposed classification scheme we study the distributions of zeros of Z_N for small Argon clusters as an illustrative example. Argon clusters have been extensively studied in the past [14–17]. Their thermodynamic behavior is governed by a hopping process between different isomers and "melting" [18–20]. Many indicators of "phase transitions" in Argon clusters have been investigated, e.g. the specific heat [21,22], the rms bond length fluctuation [23], and the onset of an $1/f$ -noise behavior of the potential energy in time dependent molecular dynamics simulations [24]. However, for a good reason, all these attempts lack a definite classification of the transitions taking place in these clusters. In the Ehrenfest sense of phase transition small clusters cannot exhibit phase transitions and the best one can say is for example that the transition exhibited by clusters approaches a first order phase transition with growing particle number N . Our approach is quite different from that point of view. Instead of trying to generalize the phase behavior of a given species for all N or trying to extract a particle number dependent behavior, we emphasise that each cluster size draws its own very specific picture. Fig. 2 displays contour plots of the scaled partition function

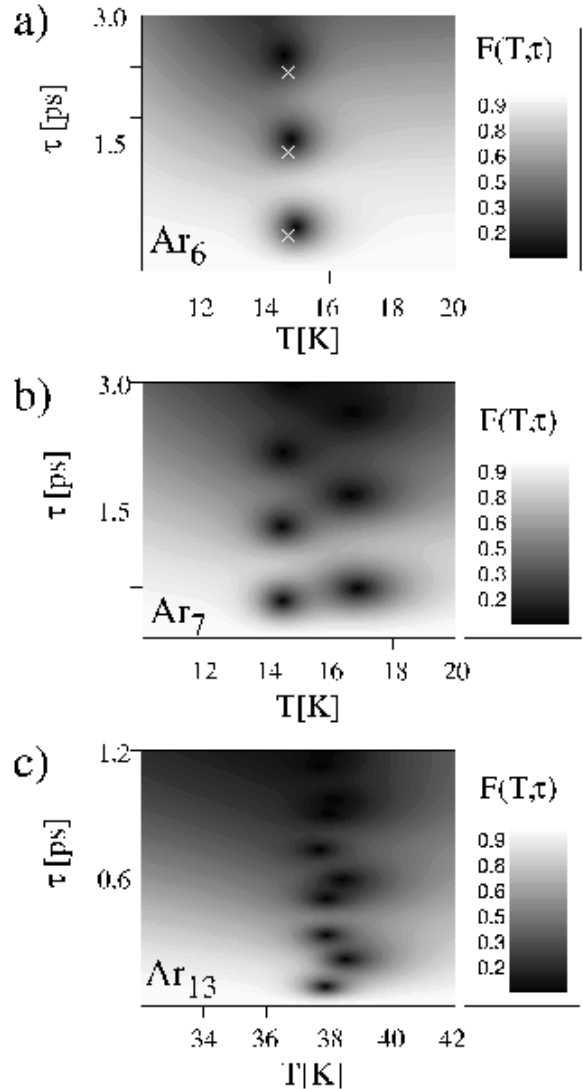


FIG. 2. Contour plots of the scaled canonical partition function in the complex temperature of a) Ar_6 , b) Ar_7 , and c) Ar_{13} calculated from Monte Carlo simulations. Dark regions indicate the locations of zeros. The crosses in the plot for Ar_6 indicate the zeros calculated with the Multiple Normal Modes model.

$$F(T, \tau) = \frac{|Z(\beta + i\tau/\hbar)|}{|Z(\beta)|} \quad (6)$$

for Ar_6 , Ar_7 , and Ar_{13} . Dark regions indicate the locations of zeros. These plots have been calculated with extensive classical Monte Carlo simulations. We utilized the multiple histogram method of Ferrenberg [25] to calculate the classical density of states used in (5). For Ar_6 which has only two significant isomers, namely the octaeder and the tri-tetraeder [26], we were able to confirm our results with the analytical Multiple-Normal-Modes (MNM) model [27]. These zeros calculated for a control of our results are indicated by crosses in Fig. 2 a). In all

cases the zeros occur within temperature ranges comparable to those given in previous publications [18,19] for the "isomer hopping" or "melting" region. Compared to the corresponding infinite system, where all zeros lie on a dense line, there are two major differences. The spacing $\Delta\tau$ between the zeros becomes discrete and, in the case of larger clusters (see Fig. 2 b-c)), a number of lines, each representing another isomer can be identified. Compared to the wealth of information given by the DOZ the extractable information from thermodynamic quantities like the specific heat is quite poor. For Ar₇ the DOZ displays that two distinct transitions with different critical temperatures β_C and different time scales $\Delta\tau$ occur between 14 and 20 K.

The MNM-model [27] mentioned above can be used to get further insight into the nature of the zeros. Within this model the partition function for a two-isomer system can be written as

$$Z(\mathcal{B}) = \sigma_1 \exp(-\mathcal{B}E_1) \prod_{i=1}^{3N-6} \frac{2\pi}{\mathcal{B}\omega_i^1} \quad (7)$$

$$+ \sigma_2 \exp(-\mathcal{B}E_2) \prod_{i=1}^{3N-6} \frac{2\pi}{\mathcal{B}\omega_i^2} ,$$

where the E_j are the ground state energies, the σ_j are the permutational degeneracies, and the ω_i^j are the vibrational eigenfrequencies of the isomers. The calculation of the zeros is straightforward and yields

$$\mathcal{B}_k = \frac{1}{\Delta E} \ln \left(\frac{\gamma_2}{\gamma_1} \right) + i \frac{(2k+1)\pi}{\Delta E} , \quad (8)$$

with $\Delta E = E_2 - E_1$, $\gamma_j = \sigma_j \prod_i 2\pi/\omega_i^j$, and $k \in \mathbb{Z}$. In this model all zeros are located on a straight line perpendicular to the real axis. The critical temperature β_C depends on the energy difference between the isomers and the vibrational entropies of both isomers. Surprisingly, the imaginary part of the zeros depends only on ΔE . The imaginary part τ_1 of the zero closest to the real axis is the inverse of the frequency ν associated with the energy difference ΔE between both isomers. One has to note, that the absolute energy difference ΔE and not the energy difference per particle $\Delta E/N$ enters here. Under the simplest assumption that the energy difference between the two phases grows proportional to N , the zeros approach the real axis with $1/N$.

It is now straightforward to expand the classification scheme given by Grossmann *et al.* to finite systems. The discreteness of the DOZ in finite systems requires a redefinition of the parameters α and γ and the definition of a new parameter reflecting the spacing between adjacent zeros. We define the discrete density of zeros at the k 'th zero as

$$\phi(\tau_k) = \frac{1}{2} \left(\frac{1}{|\mathcal{B}_k - \mathcal{B}_{k-1}|} + \frac{1}{|\mathcal{B}_{k+1} - \mathcal{B}_k|} \right) . \quad (9)$$

The parameter α is now determined by a power law fit $\phi(\tau_k) \approx \tau^\alpha$ in the region of small positive τ . The crossing angle $\nu = \arctan(\gamma)$ is defined as the angle between the straight line \mathcal{L} connecting \mathcal{B}_1 and \mathcal{B}_2 and the imaginary axis. The determination of the critical temperature β_C is more subtle. Either the crossing point of \mathcal{L} with the real axis or the real part of \mathcal{B}_1 seem to be appropriate. Obviously, in the thermodynamic limit these definitions of α , γ , and β_C are consistent with those given by Grossmann. With this definition the spacing between zeros is conveniently reflected by τ_1 , which has in the quantum mechanical case a simple straightforward interpretation. By going from real temperatures $\beta = 1/(k_B T)$ to complex temperatures $\beta + i\tau/\hbar$ the quantum mechanical partition function can be written as

$$Z(\beta + i\tau/\hbar) = \text{Tr} \langle \exp(-\tau H/\hbar) \exp(-\beta H) \rangle \quad (10)$$

$$= \langle \Psi_{\text{can}} | \exp(-i\tau H/\hbar) | \Psi_{\text{can}} \rangle \quad (11)$$

$$= \langle \Psi_{\text{can}}(t=0) | \Psi_{\text{can}}(t=\tau) \rangle ,$$

introducing an (artificial) *canonical state*

$$| \Psi_{\text{can}} \rangle = \sum_i \exp \left(-\frac{\beta}{2} \epsilon_i \right) | \phi_i \rangle , \quad (12)$$

which is the sum of all eigenstates of the system appropriately weighted by the Boltzmann factor. Within this picture a zero of the partition function occurs at times τ_1 where the overlap of a time evolved canonical state and the initial state vanishes. This resembles to a correlation time, but some care is in order here. The time τ_1 is not connected to a single system, but to an ensemble of infinitely many identical systems, with a Boltzmann distribution of initial states. Thus, the times τ_1 are those times after which the whole ensemble loses its memory.

Applying this scheme to Ar₆ an analysis of Fig. 2 a) yields ($\alpha \approx 0, \gamma \approx 0, \tau_1 \approx 0.6$ ps) and a critical temperature $T_C \approx 15$ K. Thus, the isomer hopping between the octahedral and the tri-tetrahedral structure resembles a first order phase transition with a time scale $\tau_1 = 0.6$ ps. In Ar₇ two first order phase transition at $T_C = 16.2$ K and $T_C = 19.0$ K with time scales $\tau_1 = 0.4$ ps and $\tau_1 = 0.6$ ps occur. Ar₇ has three stable isomers, namely the pentagonal bi-pyramid, the single-decorated octahedron and the tetra-tetrahedron [26]. As expected, due to the greater number of isomers the DOZ for Ar₁₃ is even more complicated. It should be noted that τ_1 decreases with increasing particle number. However, because of shell effects one can not expect that the relation between the particle number and τ_1 is given by a simple power law.

As an example for a higher order phase transition we consider N bosons in a harmonic isotropic 3 dimensional trap ($\hbar = k_B = m = \omega = 1$). For non-interacting bosons the canonical partition function can be evaluated by a simple recursion [28,29]

$$Z_N(\beta) = \frac{1}{N} \sum_{k=1}^N Q_k(\beta) Z_{N-k}(\beta) , \quad (13)$$

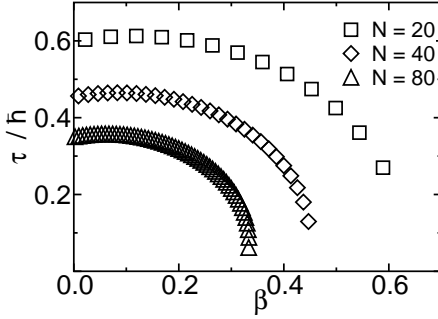


FIG. 3. Distribution of zeros for Bose-Einstein condensates in a 3d isotropic harmonic trap for $N = 20, 40$ and 80 particles.

where $Q_k(\beta) = Z_1(k\beta) = \sum_i \exp(-k\beta\epsilon_i)$ is the one-particle partition function at temperature $k\beta$ and $Z_0(\beta) = 1$. Fig. 3 displays the distributions of zeros for $N = 20, 40$, and 80 . The classification parameters are ($\alpha \approx 1.01, \gamma \approx -0.5, \tau_1 \approx 0.27$) for $N = 20$, ($\alpha \approx 1.02, \gamma \approx -0.2, \tau_1 \approx 0.13$) for $N = 40$, and ($\alpha \approx 1.01, \gamma \approx 0.02, \tau_1 \approx 0.06$) for $N = 80$ indicating a second order phase transition in all cases. A detailed analysis of the scaling behavior of τ_1 as a function of N and the dependence on the dimensionality of the trap will be given elsewhere.

A direct experimental measurement of the DOZ seems to be quite difficult, but information about the approximate location of the zeros can be retrieved by measurement of the caloric curve or the specific heat over a wide temperature range along with a parameter fit using equations (2) or (3) considering only a few zeros. In the case of small systems with a large spacing between zeros this procedure should produce adequate results. For Ar_6 we reproduced the location of the first three zeros with such a procedure with high accuracy.

In conclusion we have found, that the DOZ of the canonical partition function can be used to classify phase transitions in finite systems. The DOZ of a specific system acts like a unique fingerprint. The classification scheme given above is equivalent to that given by Grossmann *et al.* extended to the region of finite particle numbers.

We would like to thank E.R. Hilf, J. Harting, and H. Stamerjohanns for stimulating discussions.

and Critical Phenomena, (Springer, Berlin, 1984).

- [5] C. Ellert, M. Schmidt, T. Reiners, H. Haberland, Z. Phys. **D 39**, 317 (1997).
- [6] P. Borrmann *et al.*, to be published in: J. Chem. Phys. (1999).
- [7] C. N. Yang and T. Lee, Phys. Rev. **97**, 404 (1952).
- [8] C. N. Yang and T. Lee, Phys. Rev. **87**, 410 (1952).
- [9] S. Grossmann and W. Rosenhauer, Zeitschrift für Physik **207**, 138 (1967).
- [10] S. Grossmann and W. Rosenhauer, Zeitschrift für Physik **218**, 437 (1969).
- [11] S. Grossmann and V. Lehmann, Zeitschrift für Physik **218**, 449 (1969).
- [12] Since the canonical and the microcanonical partition function are related by a Laplace transform all results given in the Letter can be easily transformed to statements for the microcanonical ensemble.
- [13] E. Titchmarsh, *The Theory of Functions* (Oxford University Press, Oxford, 1964).
- [14] R. S. Berry, J. Jellinek, and N. G., Phys. Rev. A **30**, 919 (1984).
- [15] R. S. Berry, J. Jellinek, and G. Natanson, Chem. Phys. Lett. **107**, 227 (1984).
- [16] T. Beck, J. Jellinek, and R. S. Berry, J. Chem. Phys. **87**, 545 (1987).
- [17] J. Jellinek, T. L. Beck, and R. S. Berry, J. Chem. Phys. **84**, 2783 (1986).
- [18] P. Labastie and R. L. Whetten, Phys. Rev. Lett. **65**, 1567 (1990).
- [19] D. J. Wales and R. S. Berry, J. Chem. Phys. **92**, 4283 (1989).
- [20] R. E. Kunz and R. S. Berry, Phys. Rev. E **49**, 1895 (1994).
- [21] P. Borrmann, D. Gloski, and E. Hilf, Surface Review and Letters **3**, 103 (1996).
- [22] H. Heinze, P. Borrmann, H. Stamerjohanns, and E. Hilf, Z. Phys. **D 40**, 190 (1997).
- [23] P. Borrmann, Computational Material Scienc **2**, 593 (1994).
- [24] S. K. Nayak, R. Ramaswamy, and C. Chakravarty, Phys. Rev. E **51**, 3376 (1995).
- [25] A. M. Ferrenberg and R. H. Swendsen, Phys. Rev. Lett. **63**, 1195 (1989).
- [26] M. R. Hoare, Advances in Chemical Physics **40**, 49 (1979).
- [27] G. Franke, E. Hilf, and P. Borrmann, J. Chem. Phys. **98**, 3496 (1993).
- [28] P. Borrmann, G. Franke, J. Chem. Phys. **98**, 2484 (1993).
- [29] P. Borrmann, J. Harting, O. Mülken, and E. Hilf, Phys. Rev. A **60**, 1519 (1999).

[1] R. Berry, Nature **393**, 212 (1998).

[2] M. Schmidt, B. von Issendorf, and H. Haberland, Nature **393**, 238 (1998).

[3] A. Proykova, R.S. Berry, Z. Phys. **D 40**, 215 (1997).

[4] O.G. Mouritsen, *Computer Studies of Phase Transitions*